Journal of Oleo Science
Copyright ©2013 by Japan Oil Chemists' Society
J. Oleo Sci. **62**, *(7) 471-480 (2013)*

Miscibility of Egg Yolk Lecithin with Palmitic Acid and Hexadecanol at the Air-Water Interface

Hiromichi Nakahara and Osamu Shibata*

Department of Biophysical Chemistry, Faculty of Pharmaceutical Sciences, Nagasaki International University; 2825-7 Huis Ten Bosch, Sasebo, Nagasaki 859-3298, Japan

Abstract: The miscibility of Langmuir monolayers of egg yolk lecithin (eggPC) with *n*-hexadecanoic acid (PA), 1-hexadecanol (HD), and their equimolar mixture (PA/HD) was investigated thermodynamically and morphologically. Surface pressure (π)-molecular area (A) and surface potential (ΔV)-A isotherms for the binary and ternary systems were measured, employing the Wilhelmy method and the ionizing ^{241}Am electrode method, respectively. From the thermodynamic perspective, eggPC was partially miscible with PA, HD, and PA/HD within the monolayer state, in terms of an excess Gibbs free energy of mixing calculated from the π-A isotherms and a two-dimensional phase diagram based on a monolayer collapse pressure. This was also directly supported by phase behavior observations using fluorescence microscopy (FM). EggPC formed a typical liquid-expanded (LE) monolayer, and the others formed liquid-condensed (LC) monolayers. The FM images exhibited miscible modes at middle molar fractions of PA, HD, and PA/HD, and immiscible patterns at large molar fractions for all the systems examined. A new finding in the present study was that the eggPC/PA, eggPC/HD, and eggPC/(PA/HD) systems exhibited partial miscibility, although the systems were made of both LE (eggPC) and LC monolayers (the others). This miscibility is considered to be attributable to the molecular species comprising eggPC.

Key words: Langmuir monolayer, EggPC, Palmitic acid, Hexadecanol, Surface pressure, Surface potential

1 INTRODUCTION

Pulmonary surfactants, lipid-protein complexes secreted from alveolar type II cells, are essential for the maintenance of respiration in human beings and animals. Their main function is to reduce the surface tension of the alveoli[1]. An infant with a native lack of pulmonary surfactants suffers neonatal respiratory distress syndrome (NRDS). The artificial pulmonary surfactant preparation, Surfacten®, a bovine-derived pulmonary surfactant extract supplemented with dipalmitoylphosphatidylcholine (DPPC), palmitic acid (PA), and tripalmitin, is used in Japan as a first-line treatment for NRDS. In addition, many medical doctors have recognized the possibility of applying pulmonary surfactants to a wide range of pulmonary diseases. However, the current preparation is expensive, such that the application of Surfacten® only in NRDS is covered by health insurance in Japan. A further complication stems from the risk of anthropozoonosis. As the development of a lower cost preparation with fewer side effects is necessary, synthetic preparations which are not derived from animal sources have been extensively investigated. These can be classified into two types: protein (or peptide)-free preparations (e.g., Exosurf®)[2-4] and protein (peptide)-containing preparations (e.g., Surfaxin®)[5-7]. Indeed, the protein (peptide)-containing preparation is currently under investigation with the aim of developing effective treatments for NRDS and other conditions. As replacements of the lipid components in pulmonary surfactants, DPPC, phosphatidylglycerol (PG), PA, and hexadecanol (HD) are often utilized[4, 6, 8, 9]. Further examples, such as KL_4[10, 11], rSP-C[12, 13], and Hel 13-5 peptides[14-16], are also under consideration as protein (or peptide) mimics of natural SP-B and SP-C proteins, which are the hydrophobic proteins in pulmonary surfactants.

As a biophysical function, pulmonary surfactant preparations must form a stable monolayer that can reduce the surface tension nearly to zero at the air-alveolar fluid interface during expiration[17]. The stability is also deeply related to the prevention of alveolar collapse during periods of lung compression[17]. It is widely accepted that these functions are primarily induced by phospholipids (particularly DPPC) in pulmonary surfactants. However, the convention-

*Correspondence to: Osamu Shibata, Department of Biophysical Chemistry, Faculty of Pharmaceutical Sciences, Nagasaki International University; 2825-7 Huis Ten Bosch, Sasebo, Nagasaki 859-3298, Japan
E-mail: wosamu@niu.ac.jp
Accepted February 13, 2013 (received for review January 5, 2013)
Journal of Oleo Science ISSN 1345-8957 print / ISSN 1347-3352 online
http://www.jstage.jst.go.jp/browse/jos/ http://mc.manusriptcentral.com/jjocs

al artificial pulmonary surfactant preparation, which is contains DPPC as its main component, is considered to be prohibitively expensive for extending its application to other pulmonary diseases. In fact, the drug cost of Surfaxin®, the first FDA-approved peptide-containing synthetic surfactant, amounts to about $700 per infant treated. Surfaxin® is formulated as an 8.5 mL intratracheal suspension in a glass vial. According to Discovery Laboratories, Inc. (PA, USA), each milliliter contains 30 mg phospholipids [22.50 mg DPPC and 7.50 mg palmitoyloleoylphosphatidylglycerol sodium salt (POPG, Na)], 4.05 mg PA, and 0.862 mg KL_4. Thus, Surfaxin® consists mainly of DPPC. Considering also the drug cost of Surfacten® (～￥100,000), the synthetic-surfactant types of RDS drugs obviously have not achieved extensive cost reductions for RDS treatments. This shortcoming, related to the high production costs of DPPC, prompted our exploration for a DPPC alternative. In the present study, we targeted virus-free egg yolk phosphatidylcholine (eggPC), extracted and purified from relatively less expensive egg yolk lecithin. DPPC possesses double saturated hydrocarbon chains (2C16:0). Similarly, the fatty acid moieties in eggPC are double hydrocarbon chains, comprising combinations of both saturated and unsaturated acyl chains. Thus, we considered PA (C16:0) and HD (C16:0) as materials complementary to the degree of saturation in eggPC.

In a first approach, we considered two-dimensional (2D) monolayers at the air-water interface to investigate the physicochemical interactions of eggPC with PA, HD, and an equimolar PA/HD mixture. The only structural difference between PA and HD is their head group; their monolayer properties are very similar. Thus, in this study, the composition of the PA/HD mixture was kept constant at a 1:1 molar ratio. Our objective was to elucidate the miscibility, interactions, and phase behaviors of the binary and ternary mixtures. The interfacial behaviors of eggPC with PA, HD, and their equimolar mixture in the monolayer state were evaluated by surface pressure (π)-molecular area (A) and surface potential (ΔV)-A isotherms on 0.15 M NaCl at 298.2 K. The excess Gibbs free energy of mixing was calculated from the isotherm data, and a 2D phase diagram was constructed from the monolayer collapse pressures. In addition, the phase behaviors for the monolayers upon compression were examined using *in situ* fluorescence microscopy (FM).

2 EXPERIMENTAL

2.1 Materials

Egg yolk lecithin PC-98N (>98% phosphatidylcholine; virus-free; lot# AT2002), abbreviated as eggPC, was a gift from the Kewpie Corporation Fine Chemical Division (Tokyo, Japan). n-Hexadecanoic acid (also known as palmitic acid (PA); 99%) was purchased from Sigma-Aldrich Co. (St. Louis, MO). 1-Hexadecanol (palmityl alcohol (HD); >99%) was obtained from nacalai tesque (Kyoto, Japan). 3,6-Bis (diethylamino)-9-(2-octadecyloxycarbonyl) phenyl chloride (R18) from Molecular Probes Inc. (Eugene, OR) was employed as a fluorescent probe. These lipids were used without further purification. n-Hexane (98.5%) and ethanol (99.5%) were purchased from Merck (Uvasol®, Darmstadt, Germany) and nacalai tesque, respectively. A 9:1 v/v n-hexane/ethanol mixture was used as a spreading solvent. Sodium chloride (nacalai tesque) was roasted at 1023 K for 24 h to remove all surface-active organic impurities. The substrate solution was prepared using thrice-distilled water (surface tension = 72.0 mN m^{-1} at 298.2 K; electrical resistivity = 18 MΩ cm).

2.2 Methods

2.2.1 Surface pressure-area isotherms

The surface pressures (π) of the monolayers were measured using an automated homemade Wilhelmy balance. The surface pressure balance (Mettler Toledo, AG-64) had a resolution of 0.01 mN m^{-1}. The pressure-measuring system was equipped with filter paper (Whatman 541, periphery = 4 cm). The trough was made from Teflon®-coated brass (area = 750 cm^2), and Teflon® barriers (both hydrophobic and lipophobic) were used in this study. Surface pressure (π)-molecular area (A) isotherms were recorded at 298.2 ± 0.1 K. Stock solutions of eggPC (1.3 mM), PA (1.3 mM), and HD (1.3 mM) were prepared in n-hexane/ethanol (9:1 v/v). The spreading solvents were allowed to evaporate for 15 min prior to compression. The monolayer was compressed at a speed of ～0.10 nm^2 $molecule^{-1}$ min^{-1}. The standard deviations (SD) for molecular surface area and surface pressure were ～0.01 nm^2 and ～0.1 mN m^{-1}, respectively[14, 18, 19].

2.2.2 Surface potential-area isotherms

The surface potential (ΔV) was recorded simultaneously with surface pressure, when the monolayer was compressed and expanded at the air-water interface. It was monitored with an ionizing ^{241}Am electrode at 1－2 mm above the interface, while a reference electrode was dipped in the subphase. An electrometer (Keithley 614) was used to measure the surface potential. The SD for the surface potential was 5 mV[20, 21].

2.2.3 Fluorescence microscopy (FM)

Fluorescence microscopic (U.S.I. System BM-1000) observations and compression isotherm measurements were carried out simultaneously. A spreading solution of the surfactants was prepared as a mixed solution doped with 1 mol% fluorescence probe (R18). A 300 W xenon lamp (XL 300, Pneum) was used for the excitation of the FM probe. Excitation and emission wavelengths were selected by an appropriate beam splitter/filter combination (Mitutoyo band path filter = 546 nm; Olympus cut filter = 590 nm). The

monolayer was observed using a 20-fold magnification of a long-distance objective lens (Mitutoyo, f = 200/focal length = 20 mm). Fluorescent micrographs were recorded with a video camera (757 JAI ICCD camera, Copenhagen, Denmark) connected to the microscope, directly into computer memory via an on-line image processor (VAIO PCV-R53 Sony, Video Capture Soft). The entire optical setup was placed on an active vibration isolation unit (model-AY-1812, Visolator, Meiritz Seiki Co. Ltd., Yokohama, Japan)[22,23].

3 RESULTS AND DISCUSSION

3.1 π-*A* and ΔV-*A* isotherms

The surface pressure (π)-molecular area (A) and surface potential (ΔV)-A isotherms for the two-component eggPC/PA and eggPC/HD systems and for the three-component eggPC/(PA/HD) (1:1 mol/mol) system on 0.15 M NaCl at 298.2 K are shown in Fig. 1. Note that eggPC is highly purified lecithin made from fresh egg yolk, but is a molecular species containing the following fatty acid moieties: 32.0% C16:0, 1.2% C16:1, 12.7% C18:0, 30.0% C18:1, 14.8 % C18:2, 4.0% C20:4, 1.2% C22:6, and 4.2% others. Under the present experimental conditions, eggPC formed a typical liquid-expanded (LE) monolayer (*curve 1* in Fig. 1A), due to its unsaturated acyl chain content (>51.2%). The collapse pressure (π^c) of the eggPC monolayer was ~ 46 mN m^{-1} at 0.52 nm^2. The extrapolated area of highly-packed states on the π-A isotherm was 0.75 nm^2, partially a result of the low packing because of the unsaturated hydrophobic chains. PA (*curve 7* in Fig. 1A) formed a liquid-condensed (LC) monolayer with π^c = ~56 mN m^{-1} (0.16 nm^2). In addition, the PA monolayer had a transition from the LC state to the solid state at ~20 mN m^{-1}. A limiting molecular area (or extrapolated area) of PA monolayers was ~0.19 nm^2, which was based on the cross-sectional area of the saturated aliphatic chains (C16:0). The isotherm of the PA monolayers agreed well with previously reported data[24,25]. In the binary eggPC/PA system (Fig. 1A), the π-A isotherms shifted to smaller areas with increasing molar fractions of PA (X_{PA}). A plateau region near the π^c of the eggPC monolayers was observed at X_{PA} = 0.7 (*curve 5*) and 0.9 (*curve 6*). At the plateau, eggPC monolayers were considered to be collapsing and becoming other three-dimensional states such as bilayers and multilayers. Then, the isotherms underwent a second monolayer collapse near the π^c of the PA monolayers upon further compression. This behavior suggested the immiscibility of the eggPC and PA, which will be discussed in more detail later. The surface potential (ΔV) value corresponds to a dipole moment in the direction of a surface normal for monolayer-forming molecules. That is, the value reflects the monolayer orientation upon compression. All the compounds used in the present study are typical hydrocarbons rather than fluorocarbons. Thus, herein, a positive increment in ΔV indicates an improvement of the monolayer orientation and packing upon compression. The ΔV-A isotherms exhibited sharp jumps of 130–220 mV in the vicinities of the onsets of the corresponding π-A isotherms, where π values began to increase from zero. The magnitude of the jump decreased gradually with increasing X_{PA}. The ΔV jump at small X_{PA} indicated the transi-

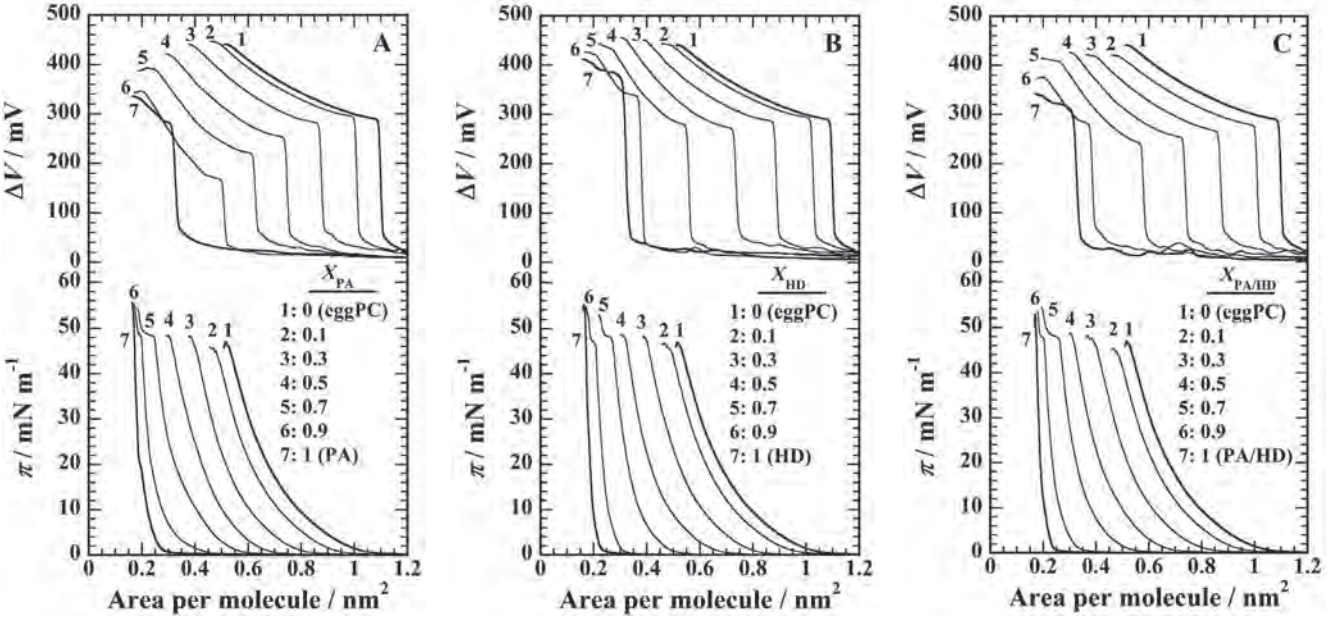

Fig. 1 The π-A and ΔV-A isotherms of the eggPC/PA (A), eggPC/HD (B), and eggPC/(PA/HD) (1:1 mol/mol) (C) monolayers on 0.15 M NaCl at 298.2 K.

tion from the gaseous to the LE phases, whereas, at large X_{PA}, it reflected the transition from the gaseous to the LC phases. As for the ΔV jump at middle X_{PA}, the transition from the gaseous to the coexistent LE/LC phases was considered to have occurred. This transition was morphologically revealed by fluorescence microscopy (*vide infra*). After the transitions, the ΔV value increased monotonously upon compression and then retained almost constant values above each π^c. The maximum ΔV values at the close-packed state apparently did not change linearly against X_{PA}. This positive variation in maximum ΔV value suggested that orientation of the lowly packed eggPC monolayers was enhanced by the addition of PA molecules.

As seen in Fig. 1B, HD (*curve 7*) formed a typical LC monolayer with $\pi^c = \sim 55$ mN m^{-1} (0.17 nm^2). Its limiting area was 0.19 nm^2. In comparison to the PA monolayers (*curve 7* in Fig. 1A), HD was found to easily form a more condensed monolayer in the slope and the onset of its π-A isotherm. This resulted from the structural difference in the head groups of PA and HD. It was very clear that the carboxyl group of PA was partially dissociated under the experimental conditions (subphase pH = ~6)[26]. Therefore, an electrostatic repulsive force among the carboxylate ions disturbed the packing of the PA hydrocarbon chains upon compression. In contrast, the HD head group is a hydroxyl group, and thus, HD monolayers can be more ordered. An equimolar mixture of PA and HD (*curve 7* in Fig. 1C) also formed LC monolayers with $\pi^c = \sim 53$ mN m^{-1} (0.17 nm^2). The π-A isotherm for the equimolar PA/HD monolayer resembled that for HD (*curve 7* in Fig. 1B), while the ΔV-A isotherm was similar to that for PA (*curve 7* in Fig. 1A). As for the binary eggPC/HD (Fig. 1B) and ternary eggPC/(PA/HD) systems (Fig. 1C), the π-A isotherms shifted to smaller areas with increasing molar fractions of HD (X_{HD}) or the PA/HD mixture ($X_{PA/HD}$). Similarly to the eggPC/PA system, plateau regions were observed at X_{HD} (or $X_{PA/HD}$) = 0.7 (*curve 5*) and 0.9 (*curve 6*). Therefore, it is suggested that eggPC was also immiscible with HD and the PA/HD mixture. In the case of the ΔV-A isotherms, a similar behavior to the eggPC/PA system was observed in Figs. 1B and 1C. However, the decrease in the degree of the ΔV jump against X_{HD} (or $X_{PA/HD}$) was not as large compared to the eggPC/PA system. On the contrary, the jump in ΔV-A isotherms at X_{HD} and $X_{PA/HD}$ = 0.9 (*curve 6*) became larger in magnitude, approaching the degree of the ΔV jump for HD and the PA/HD mixture, respectively. This recovery did not occur for the monolayer at X_{PA} = 0.9 (*curve 6* in Fig. 1A), which may be interpreted as the orientational disturbance originating from the repulsive interaction among the carboxylate groups of the PA molecules.

3.2 Excess Gibbs free energy

The π-A isotherms for the present systems (Fig. 1) can be also analyzed from a thermodynamic perspective in terms of excess Gibbs free energy of mixing (ΔG_{mix}^{exc}). The ΔG_{mix}^{exc} value is calculated from the following equation (Eq. (1))[27],

$$\Delta G_{mix}^{exc} = \int_0^{\pi} (A_{12} - X_1 A_1 - X_2 A_2)\, d\pi \qquad (1)$$

where A_i and X_i are the molecular area and molar fraction of component i, respectively, and A_{12} is the mean molecular area in the binary or ternary monolayer. For identical interactions between the two components, the value of ΔG_{mix}^{exc} is zero, which means that they are ideally mixed in the mono-

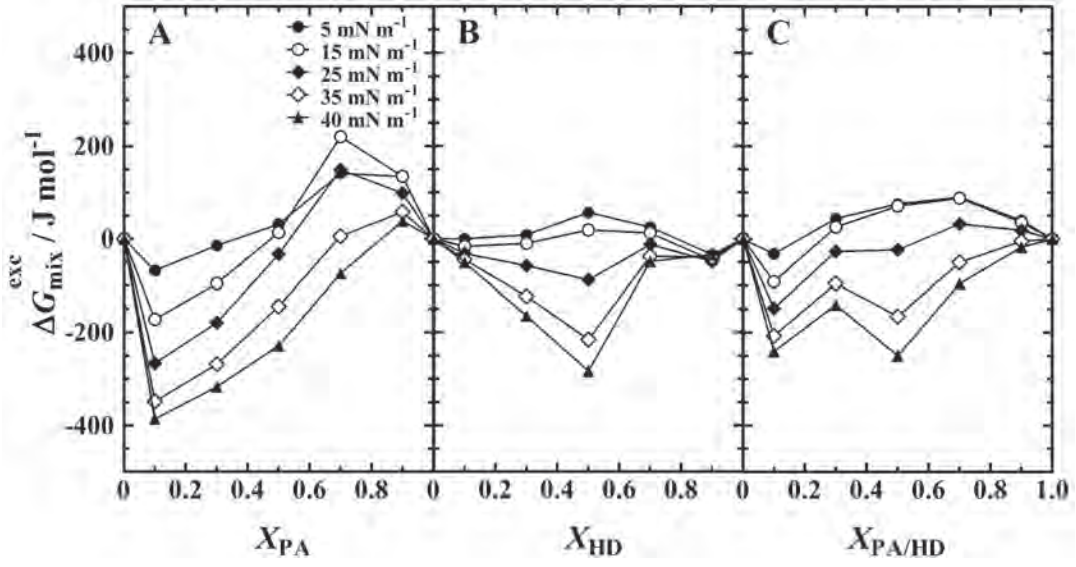

Fig. 2 Excess Gibbs free energy of mixing (ΔG_{mix}^{exc}) of the eggPC/PA (A), eggPC/HD (B), and eggPC/(PA/HD) (1:1 mol/mol) (C) monolayers as a function of X_{PA}, X_{HD}, and $X_{PA/HD}$ at representative surface pressures on 0.15 M NaCl at 298.2 K, respectively.

layer or that they are immiscible[28, 29]. A negative deviation from ideality indicates an attractive interaction between two components. The variations of ΔG_{mix}^{exc} for the eggPC/PA, eggPC/HD, and eggPC/(PA/HD) monolayers against X_{PA}, X_{HD}, and $X_{PA/HD}$ at representative surface pressures are shown in Fig. 2, respectively. In the binary eggPC/PA system (Fig. 2A), the ΔG_{mix}^{exc} value decreased with increasing surface pressure. Notably, the values at $X_{PA} = 0.1$ reached approximately -390 J mol^{-1} as a minimum at 40 mN m^{-1}. This behavior suggested that the attractive force between eggPC and PA increased upon compression, and their affinity reached a maximum at $X_{PA} = 0.1$. On the other hand, the minimum ΔG_{mix}^{exc} values were about -280 J mol^{-1} at $X_{HD} = 0.5$ for eggPC/HD (Fig. 2B), and about -240 at $X_{PA/HD} = 0.1$ and -250 J mol^{-1} at $X_{PA/HD} = 0.5$ for eggPC/(PA/HD) (Fig. 2C) at 40 mN m^{-1}. The structural difference in the head groups between PA and HD was found to be finely expressed in the ΔG_{mix}^{exc} behavior against the molar fractions. Considering the immiscibility of the present systems described above, the ΔG_{mix}^{exc} values should be nearly zero or exhibit positive deviations irrespective of molar fractions and surface pressures. However, the results in Fig. 2 suggested monolayer miscibility for these systems. This can be accounted for by the nature of the eggPC acyl chain components. In terms of chemical structures, PA and HD can interact preferentially with certain components (e.g., C16:0) in eggPC because of similarities in hydrocarbon chain lengths. Indeed, it has been reported that both PA and HD form highly ordered, nearly crystalline structures with DPPC over a wide range of PA or HD fractions[25, 26]. Lee et al. reported that the addition of PA or HD to DPPC monolayers led to the change from tilted to untilted monolayer packing because of the significantly large correlation in hydrophobic chain lengths[25]. Thus, we speculated that the ΔG_{mix}^{exc} behavior indicated partial miscibility in the present systems. The specific interaction with the component in eggPC was also observed morphologically via *in situ* fluorescence microscopy (*vide infra*).

3.3 Two-dimensional phase diagrams

For the three systems under investigation, a 2D phase diagram at 298.2 K was constructed by plotting the π^c values against the molar fractions (Fig. 3). The monolayers at X_{PA}, X_{HD}, and $X_{PA/HD} = 0.7$ and 0.9 had two π^c values. As mentioned above, the first π^c corresponded to the π^c value for eggPC monolayers and the second was attributed to the π^c values for the PA, HD, and the PA/HD monolayers. Typically, this kind of phase diagram expresses the immiscibility of the components, through the near absence of variation of π^c values against molar fractions[30, 31]. In the present study, however, the second π^c changed slightly with decreasing molar fractions; the second π^c values at $X_{PA} = 0.7$ and $X_{HD} = 0.7$ decreased by $\sim$2 mN m^{-1}, and at $X_{PA/HD} = 0.7$, it increased by $\sim$3 mN m^{-1} compared to that of PA, HD, and the PA/HD monolayers. This was also believed to result from the specific interaction of PA and HD with components (e.g., C16:0) of eggPC.

3.4 In situ FM observations

Figure 4 shows FM images for the PA, HD, and equimolar PA/HD monolayers *in situ* at the air-water interface. For the FM observations, the monolayers contained a small amount of fluorescent probe (1 mol% R18). Typically, the fluorescent probe selectively dissolves in the disordered

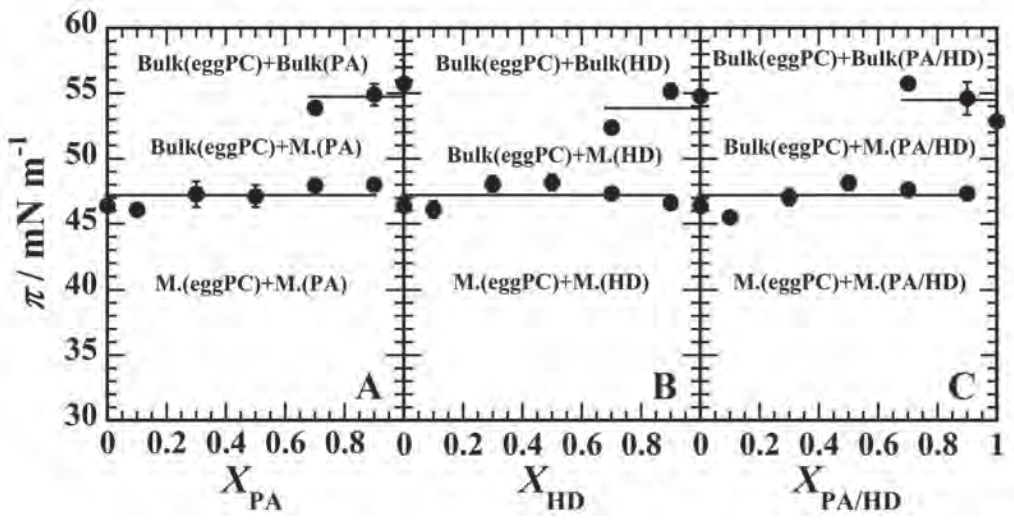

Fig. 3 Two-dimensional phase diagrams of the eggPC/PA (A), eggPC/HD (B), and eggPC/(PA/HD) (1:1 mol/mol) (C) monolayers based on the change of the collapse pressure (π^c, solid circle) on 0.15 M NaCl at 298.2 K as a function of X_{PA}, X_{HD}, and $X_{PA/HD}$, respectively. M indicates lipid monolayers, whereas Bulk denotes a solid phase of the lipids (“bulk phase” may also be called “solid phase”).

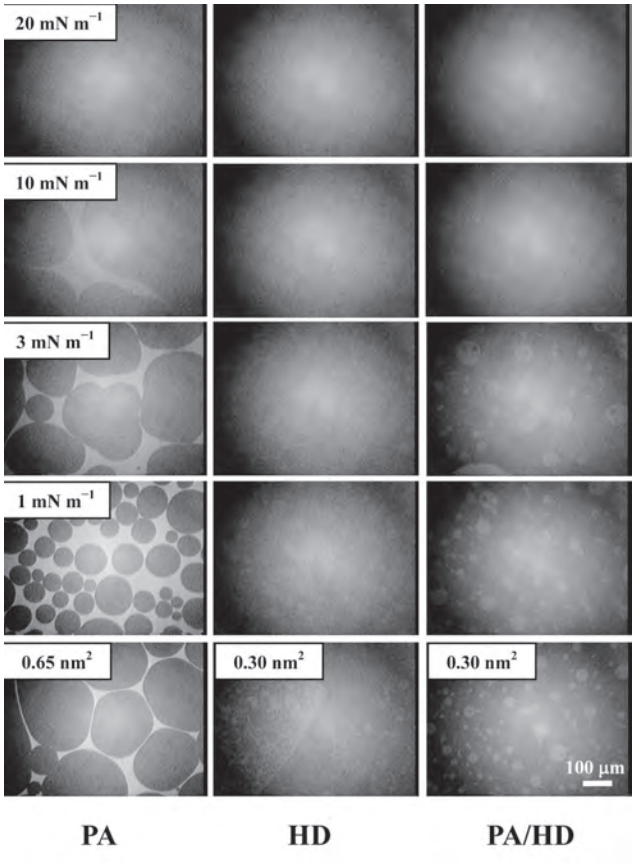

Fig. 4 FM images for single monolayers of PA, HD, and for the binary monolayer of PA/HD (1:1 mol/mol) at 0 (0.65 nm^2 for PA, and 0.30 nm^2 for HD and PA/HD), 1, 3, 10, and 20 mN m^{-1} on 0.15 M NaCl at 298.2 K. The monolayers contained 1 mol% fluorescent probe (R18). The scale bar in the lower right represents 100 μm.

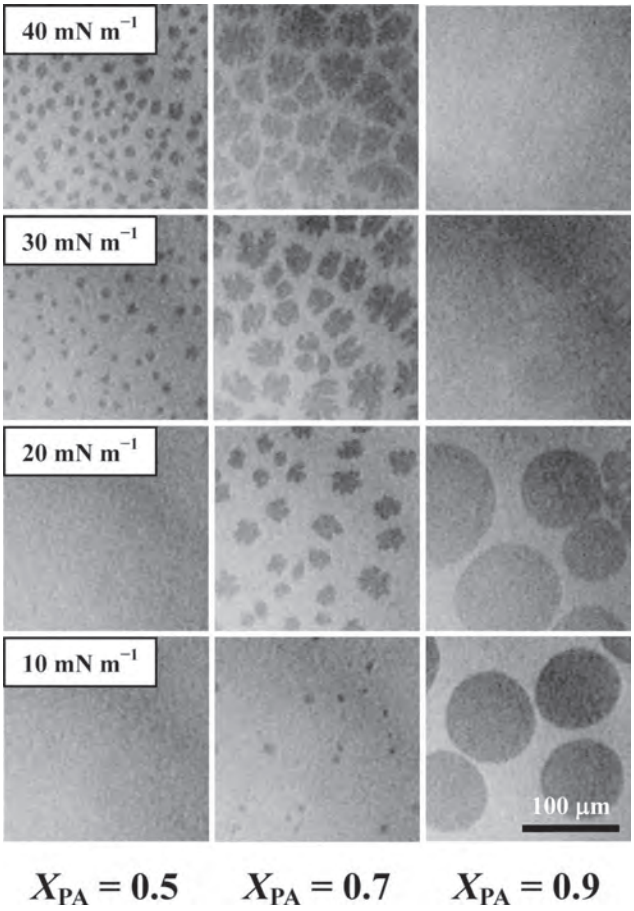

Fig. 5 FM images of the binary eggPC/PA monolayers for X_{PA} = 0.5, 0.7, and 0.9 at 10, 20, 30, and 40 mN m^{-1} on 0.15 M NaCl at 298.2 K. The monolayers contained 1 mol% fluorescent probe (R18). The scale bar in the lower right represents 100 μm.

phases of the monolayers. Bright and dark contrasts in the FM image respectively correspond to disordered and ordered phases. For the PA monolayers, the coexistence of a gaseous (bright) phase and the surface (dark, not covered by monolayers) was observed over large molecular areas, such as 0.65 nm^2. As the monolayer was compressed until $\pi = 0.1$ mN m^{-1}, the bare surface region grew steadily smaller in size and then disappeared (data not shown). After this disappearance, a similar coexistence emerged again near the onset of the π-A isotherm (see the picture at 1 mN m^{-1}). In the image, however, the dark area was assigned to the LC phase because the dark contrast grew in size with surface pressure increases from 1 to 10 mN m^{-1}. Further compression resulted in a homogeneous dark image at 20 mN m^{-1}, which corresponded to the transition to the solid phase. This agreed well with the explanation of the π-A isotherm (Fig. 1A). In the HD monolayers, the coexistence of gaseous and LC phases was observed with unclear contrast at 0.30 nm^2. With further compression to 1 mN m^{-1}, the images became homogeneously dark, and were assigned to the LC or solid phases. The dark images were observed from 1 mN m^{-1} until monolayer collapse. These results supported the formation of more condensed monolayers by HD than PA. In the case of the PA/HD mixture, the unclear coexistence images continued to be observed until ~3 mN m^{-1}, and then, they varied to the homogeneous dark image upon further compression. The FM image for single eggPC monolayers was optically and homogeneously bright over the entire range of surface pressures (data not shown) because eggPC forms a typical LE monolayer under the present conditions.

Shown in Fig. 5 are the FM images for the binary eggPC/PA monolayer. The monolayer in the range of $0 \le X_{PA} \le 0.3$ exhibited homogeneous bright images at all surface pressures (data not shown). Further addition of PA to eggPC monolayers generated coexistent dark and bright contrasts

at $X_{PA} = 0.5$ at 30 mN m^{-1}. The state of coexistence was apparently different from the above-mentioned phase states. Assuming that the coexistence comprised the gaseous/LC phases, the domain shape with dark contrast should be round because of the complete immiscibility of the two phases and the minimization of contact areas between them. Moreover, the surface pressure was too high for the gaseous/LC transition. In the present case, however, the domain was somewhat flower- or leaf-shaped. Furthermore, the domain grew in size with increasing surface pressure. This phenomenon has often been observed for a first-ordered phase transition from the LE to the LC states for typical monolayers such as dipalmitoylphosphatidylcholine and myristic acid[32, 33]. A possible explanation of this phenomenon is that a component (e.g., C16:0) in eggPC was miscible with PA because of the similarity in hydrocarbon chain lengths, and thus, the domain shape varied. The miscibility of eggPC and PA was also supported by the fact that the surface pressure for the emergence of such states of coexistence changed against X_{PA} (see the images at $X_{PA} = 0.5$ and 0.7). If the miscibility conflicted with the morphological behavior, the surface pressure of emergence should have remained constant regardless of X_{PA}. At $X_{PA} = 0.9$, the images indicated a behavior similar to PA monolayers (Fig. 4). To our knowledge, there are no reports on the present phenomenon for typical two-component systems of LE and LC monolayers. Generally, it is widely accepted that LE and LC monolayers are immiscible.

The *in situ* morphology for the binary eggPC/HD monolayer is shown in Fig. 6. As the amount of HD increased, the emergence of LC domains in the LE region occurred at $X_{HD} \geq 0.3$. The emergence was induced by the incorporation of smaller amounts of HD compared to the eggPC/PA system. This suggests the more preferable interaction of a certain component (e.g., C16:0) in eggPC with HD. The surface pressure of emergence decreased with increasing X_{HD}. The LC domain at $X_{HD} = 0.3$ and 0.5 grew larger as the surface pressure increased. The domain shape at $X_{HD} = 0.5$ resembled those of myristic acid monolayers[33]. It is generally well known that domain formation is controlled by the balance of the line tension at the boundary between the LE and LC domains and the long-range dipole-dipole interac-

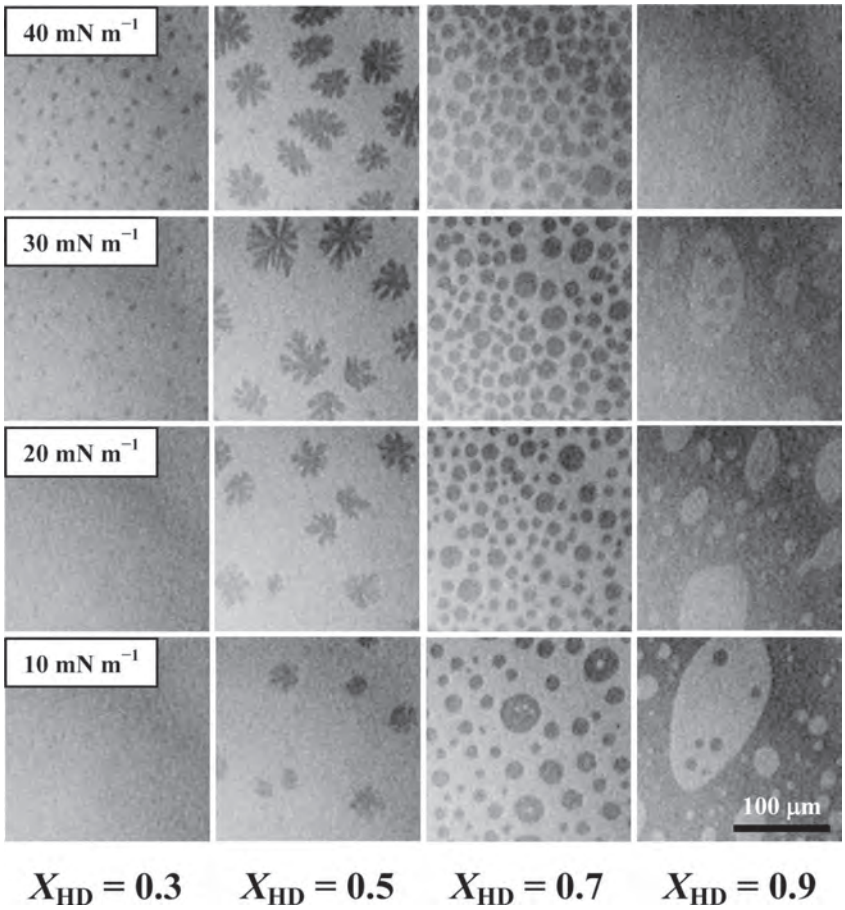

Fig. 6 FM images of the binary eggPC/HD monolayers for $X_{HD} = 0.3$, 0.5, 0.7, and 0.9 at 10, 20, 30, and 40 mN m^{-1} on 0.15 M NaCl at 298.2 K. The monolayers contained 1 mol% fluorescent probe (R18). The scale bar in the lower right represents 100 μm.

tion among LC domains[34]. For example, miscibility between the two components changes the composition in LC domains, which results in variation of the line tension. Thus, the variation in domain shape also supported the miscibility between the components. In contrast, the state of coexistence at $X_{HD} = 0.7$ was observed below a surface pressure of zero (at $A \geq 0.55$ nm^2). In addition, the LC domain did not grow in size, irrespective of the increase in surface pressure, and its appearance was round rather than leaf-shaped. This is the case of typical immiscible or phase-separated behavior. A similar morphology was observed even at $X_{HD} = 0.9$, where the phase mode resembled that of HD monolayers.

In the case of the ternary eggPC/(PA/HD) system (Fig. 7), the phase behavior was similar to the eggPC/HD system (Fig. 6) rather than the eggPC/PA system (Fig. 5), in terms of the molar fractions where LC domains appeared in the LE region and of the phase-separated morphology observed at high molar fractions. Interestingly, as opposed to the binary systems, a fusion of LC domains occurred at $X_{PA/HD} = 0.7$ (30 and 40 mN m^{-1}) and 0.9 (20 mN m^{-1}), which are indicated by white arrows in the figure. This phenomenon indicated that the phase separation was secondarily enhanced even in the immiscible FM pattern. The domain fusion may be driven by a synergistic effect of PA and HD. Nevertheless, it is suggested that eggPC was partially miscible with PA, HD, and their equimolar mixture within a monolayer.

4 CONCLUSION

PA, HD, and the equimolar mixture of PA/HD were partially miscible with eggPC in the binary and ternary monolayer states. In a strict sense, they are considered to interact favorably both thermodynamically and morphologically with certain components containing fatty acid moieties, such as C16:0 in eggPC. The 2D phase diagrams were constructed by plotting the surface pressures of monolayer collapses against X_{PA}, X_{HD}, and $X_{PA/HD}$. The monolayers at

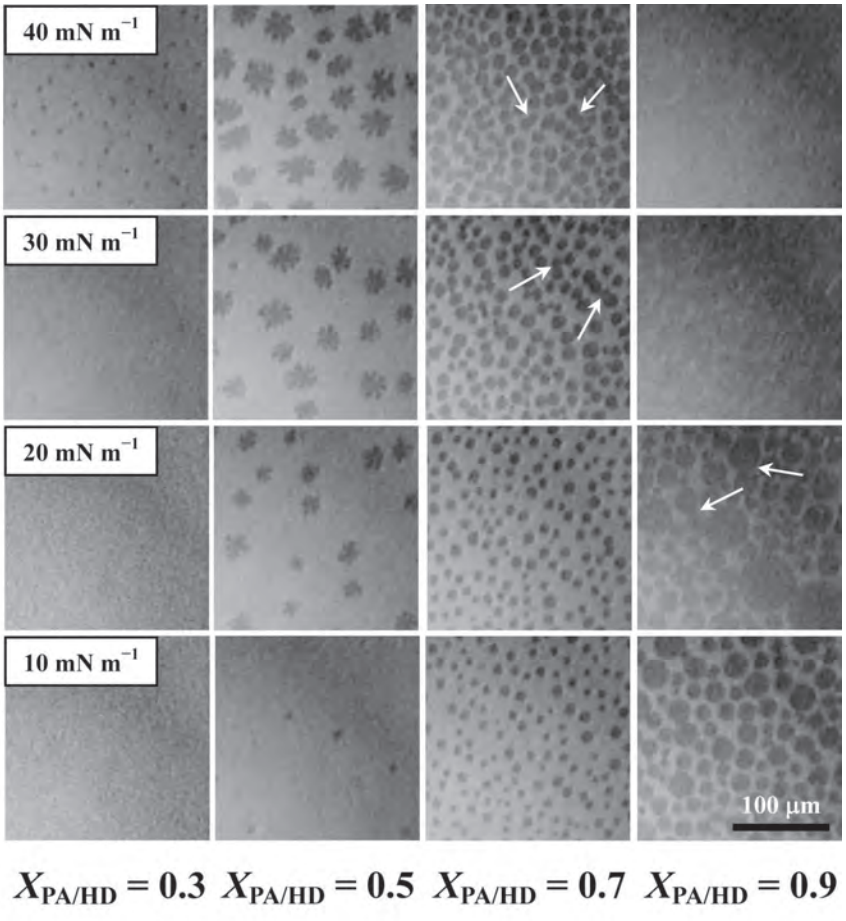

Fig. 7 FM images of the ternary eggPC/(PA/HD) (1:1 mol/mol) monolayers for $X_{PA/HD}$ = 0.3, 0.5, 0.7, and 0.9 at 10, 20, 30, and 40 mN m^{-1} on 0.15 M NaCl at 298.2 K. The monolayers contained 1 mol% fluorescent probe (R18). The scale bar in the lower right represents 100 μm.

molar fractions of 0.7 and 0.9 showed two collapse pressures on the π-A isotherms; the first corresponded to the collapse of eggPC monolayers and the second was for the other component. That is, the phase diagram obtained herein reflected the case of immiscible patterns. Notably, the second collapse pressure varied slightly against the molar fraction. In addition, the excess Gibbs free energy of mixing for the present system was calculated on the basis of the additivity rule. The Gibbs energy for all the systems indicated negative variations with increasing surface pressures at several molar fractions, which implied partial miscibility. FM observations of the phase behavior for the current monolayers morphologically supported partial miscibility on the micrometer scale. Generally, a two-component system of LE and LC monolayers produces an FM image showing phase separation, where LC domains with round shapes float in LE regions at the air-water interface. In the present systems, however, miscible morphological patterns were clearly observed over limited molar fractions [$0.5 \le X_{PA} \le 0.7$ for eggPC/PA, $0.3 \le X_{HD} \le 0.5$ for eggPC/HD, and $0.3 \le X_{PA/HD} \le 0.5$ for eggPC/(PA/HD)]: the size growth of LC domains with an increase in surface pressure and the emergence of flowerlike or leaf-like LC domains. At large molar fractions, FM images exhibited phase-separated morphologies which corresponded to the immiscibility of two components [$0.7 < X_{PA} < 1$ for eggPC/PA, $0.5 < X_{HD} < 1$ for eggPC/HD, and $0.5 < X_{PA/HD} < 1$ for eggPC/(PA/HD)]. The similarity in the hydrocarbon chain lengths among PA, HD, and the eggPC components with saturated hydrocarbons (for example, C16:0) induces the slight affinity for the systems described herein.

ACKNOWLEDGEMENTS

This work was supported by a Grant-in-Aid for Scientific Research 23510134 from the Japan Society for the Promotion of Science (JSPS). It was also supported by a Grant-in-Aid for Young Scientists (B) 25790020 from the JSPS and funding from the Foundation, Oil & Fat Industry Kaikan (H.N.).

References

1) Pérez-Gil, J.; Keough, K. M. W. Interfacial properties of surfactant proteins. *Biochim. Biophys. Acta* **1408**, 203-217 (1998).
2) Kirkness, J. P.; Eastwood, P. R.; Szollosi, I.; Platt, P. R.; Wheatley, J. R.; Amis, T. C.; Hillman, D. R. Effect of surface tension of mucosal lining liquid on upper airway mechanics in anesthetized humans. *J. Appl. Physiol.* **95**, 357-363 (2003).
3) Kirkness, J. P.; Madronio, M.; Stavrinou, R.; Wheatley, J. R.; Amis, T. C. Relationship between surface tension of upper airway lining liquid and upper airway collapsibility during sleep in obstructive sleep apnea hypopnea syndrome. *J. Appl. Physiol.* **95**, 1761-1766 (2003).
4) Pfister, R. H.; Soll, R. F. New Synthetic Surfactants: The Next Generation? *Biol. Neonate* **87**, 338-344 (2005).
5) Wiswell, T. E.; Smith, R. M.; Katz, L. B.; Mastroianni, L.; Wong, D. Y.; Willms, D.; Heard, S.; Wilson, M.; Hite, R. D.; Anzueto, A.; Revak, S. D.; Cochrane, C. G. Bronchopulmonary segmental lavage with Surfaxin (KL(4)-surfactant) for acute respiratory distress syndrome. *Am. J. Respir. Crit. Care Med.* **160**, 1188-1195 (1999).
6) Ma, J.; Koppenol, S.; Yu, H.; Zografi, G. Effects of a cationic and hydrophobic peptide, KL4, on model lung surfactant lipid monolayers. *Biophys. J.* **74**, 1899-1907 (1998).
7) Revak, S. D.; Merritt, T. A.; Cochrane, C. G.; Heldt, G. P.; Alberts, M. S.; Anderson, D. W.; Kheiter, A. Efficacy of synthetic peptide-containing surfactant in the treatment of respiratory distress syndrome in preterm infant rhesus monkeys. *Pediatr. Res.* **39**, 715-724 (1996).
8) Pérez-Gil, J.; Casals, C.; Marsh, D. Interactions of hydrophobic lung surfactant proteins SP-B and SP-C with dipalmitoylphosphatidylcholine and dipalmitoylphosphatidylglycerol bilayers studied by electron spin resonance spectroscopy. *Biochemistry* **34**, 3964-3971 (1995).
9) Tanaka, Y.; Takei, T.; Aiba, T.; Masuda, K.; Kiuchi, A.; Fujiwara, T. Development of synthetic lung surfactants. *J. Lipid Res.* **27**, 475-485 (1986).
10) Moya Fernando, R.; Gadzinowski, J.; Bancalari, E.; Salinas, V.; Kopelman, B.; Bancalari, A.; Kornacka, M. K.; Merritt, T. A.; Segal, R.; Schaber, C. J.; Tsai, H.; Massaro, J.; d'Agostino, R. A multicenter, randomized, masked, comparison trial of lucinactant, colfosceril palmitate, and beractant for the prevention of respiratory distress syndrome among very preterm infants. *Pediatrics* **115**, 1018-1029 (2005).
11) Cochrane, C. G.; Revak, S. D. Pulmonary surfactant protein B (SP-B): structure-function relationships. *Science* **254**, 566-568 (1991).
12) Grigoriev, D. O.; Kragel, J.; Akentiev, A. V.; Noskov, B. A.; Miller, R.; Pison, U. Relation between rheological properties and structural changes in monolayers of model lung surfactant under compression. *Biophys. Chem.* **104**, 633-642 (2003).
13) Krol, S.; Ross, M.; Sieber, M.; Kunneke, S.; Galla, H.-J.; Janshoff, A. Formation of three-dimensional protein-lipid aggregates in monolayer films induced by surfactant protein B. *Biophys. J.* **79**, 904-918 (2000).

14) Nakahara, H.; Lee, S.; Sugihara, G.; Shibata, O. Mode of interaction of hydrophobic amphiphilic α-helical peptide/dipalmitoylphosphatidylcholine with phosphatidylglycerol or palmitic acid at the air-water interface. *Langmuir* **22**, 5792-5803(2006).
15) Nakahara, H.; Nakamura, S.; Hiranita, T.; Kawasaki, H.; Lee, S.; Sugihara, G.; Shibata, O. Mode of interaction of amphiphilic α-helical peptide with phosphatidylcholines at the air-water interface. *Langmuir* **22**, 1182-1192(2006).
16) Nakahara, H.; Lee, S.; Sugihara, G.; Chang, C.-H.; Shibata, O. Langmuir monolayer of artificial pulmonary surfactant mixtures with an amphiphilic peptide at the air/water interface: Comparison of new preparations with Surfacten(Surfactant TA). *Langmuir* **24**, 3370-3379(2008).
17) Schürch, S.; Goerke, J.; Clements, J. A. Direct determination of surface tension in the lung. *Proc. Natl. Acad. Sci. USA* **73**, 4698-4702(1976).
18) Nakamura, S.; Nakahara, H.; Krafft, M. P.; Shibata, O. Two-component Langmuir monolayers of single-chain partially fluorinated amphiphiles with dipalmitoylphosphatidylcholine(DPPC). *Langmuir* 23, 12634-12644 (2007).
19) Nakahara, H.; Tsuji, M.; Sato, Y.; Krafft, M. P.; Shibata, O. Langmuir monolayer miscibility of single-chain partially fluorinated amphiphiles with tetradecanoic acid. *J. Colloid Interf. Sci.* **337**, 201-210(2009).
20) Nakahara, H.; Shibata, O.; Moroi, Y. Examination of surface adsorption of sodium chloride and sodium dodecyl sulfate by surface potential measurement at the air/solution interface. *Langmuir* **21**, 9020-9022 (2005).
21) Nakahara, H.; Shibata, O.; Rusdi, M.; Moroi, Y. Examination of Surface Adsorption of Soluble Surfactants by Surface Potential Measurement at the Air/Solution Interface. *J. Phys. Chem. C* **112**, 6398-6403(2008).
22) Hiranita, T.; Nakamura, S.; Kawachi, M.; Courrier, H. M.; Vandamme, T. F.; Krafft, M. P.; Shibata, O. Miscibility behavior of dipalmitoylphosphatidylcholine with a single-chain partially fluorinated amphiphile in Langmuir monolayers. *J. Colloid Interf. Sci.* **265**, 83-92(2003).
23) Nakahara, H.; Nakamura, S.; Kawasaki, H.; Shibata, O. Properties of two-component Langmuir monolayer of single chain perfluorinated carboxylic acids with dipalmitoylphosphatidylcholine(DPPC). *Colloids Surf. B* **41**, 285-298(2005).
24) Ma, G.; Allen, H. C. Condensing effect of palmitic acid on DPPC in mixed Langmuir monolayers. *Langmuir* **23**, 589-597(2007).
25) Lee, K. Y. C.; Gopal, A.; von Nahmen, A.; Zasadzinski, J. A.; Majewski, J.; Smith, G. S.; Howes, P. B.; Kjaer, K. Influence of palmitic acid and hexadecanol on the phase transition temperature and molecular packing of dipalmitoylphosphatidylcholine monolayers at the air-water interface. *J. Chem. Phys.* **116**, 774-783 (2002).
26) Nakahara, H.; Lee, S.; Shoyama, Y.; Shibata, O. The role of palmitic acid in pulmonary surfactant systems by Langmuir monolayer study: Lipid-peptide interactions. *Soft Matter* **7**, 11351-11359(2012).
27) Goodrich, F. C. In *Proceedings of the 2nd International Congress on Surface Activity*, J. H. Schulman ed., Butterworth & Co.: London, 1957; p 85.
28) Marsden, J.; Schulman, J. H. *Trans. Faraday Soc.* **34**, 748-758(1938).
29) Shah, D. O.; Schulman, J. H. J. *Lipid Res.* **8**, 215-226 (1967).
30) Nakahara, H.; Nakamura, S.; Nakamura, K.; Inagaki, M.; Aso, M.; Higuchi, R.; Shibata, O. Cerebroside Langmuir monolayers originated from the echinoderms: II. Binary systems of cerebrosides and steroids. *Colloids Surf. B* **42**, 175-185(2005).
31) Nakahara, H.; Nakamura, S.; Nakamura, K.; Inagaki, M.; Aso, M.; Higuchi, R.; Shibata, O. Cerebroside Langmuir monolayers originated from the echinoderms I. Binary systems of cerebrosides and phospholipids. *Colloids Surf. B* **42**, 157-174(2005).
32) Weis, R. M.; McConnell, H. M. Two-dimensional chiral crystals of phospholipid. *Nature* **310**, 47-49(1984).
33) Nakahara, H.; Tsuji, M.; Sato, Y.; Krafft, M. P.; Shibata, O. Langmuir monolayer miscibility of single-chain partially fluorinated amphiphiles with tetradecanoic acid. *J. Colloid Interface Sci.* **337**, 201-210(2009).
34) Möhwald, H. Phospholipid and phospholipid-protein monolayers at the air/water interface. *Annu. Rev. Phys. Chem.* **41**, 441-476(1990).